Dynamic Interactions between a Silica Sphere and Deformable Interfaces in Organic Solvents Studied by Atomic Force Microscopy

Natalie P. Kuznicki,† David Harbottle,†,‡ Jacob Masliyah,† and Zhenghe Xu*,†

†Department of Chemical and Materials Engineering, University of Alberta, Edmonton, Alberta, Canada
‡School of Chemical and Process Engineering, University of Leeds, Leeds, U.K.
* Email: zhenghe.xu@ualberta.ca (Z.X.).

ABSTRACT: Recent studies have successfully measured surface forces using 8 atomic force microscope (AFM) and modeled surface deformations using the Stokes−Reynolds−Young−Laplace (SRYL) equations for particle−droplet, particle−bubble, droplet−droplet, and bubble−bubble systems in various solutions. The current work focuses on interactions between spherical silica particles and a viscoelastic interface of water droplets in crude oil. The self-assembly of surface active natural polyaromatic molecules (NPAMs) at the oil−water interface has previously been shown to change a viscous dominant oil−water interface to an elastic dominant interface upon aging, due to gradual formation of rigid interfacial networks. AFM was used to measure the interactions between a small silica sphere (D ≈ 8 μm) and a deformable water droplet (D ≈ 70 μm), which exhibits time-dependent interfacial viscoelasticity in NPAM solutions. Unlike the systems studied previously, the measured deformation shown as a repulsive force over the region of constant compliance could not be modeled adequately by the conventional SRYL equations which are applicable only to purely Laplacian interfaces. As the water droplet ages in NPAM solutions, a rigid "skin" forms at the oil−water interface, with the interface exhibiting increased elasticity. Over a short aging period (up to 15 min in NPAM-in-toluene solution), interfacial deformation is well predicted by the SRYL model. However, upon further exposure to the NPAM solution, droplet deformation is over predicted by the model. Physical properties of this mechanical barrier as a function of interfacial aging were further investigated by measuring interfacial tension, dilatational rheology, and interfacial "crumpling" (non-smooth, non-Laplacian interface) upon droplet volume reduction. By introducing a viscoelasticity parameter to account for interfacial stiffening and using experimentally determined elasticity, we are able to correct this discrepancy and predict droplet deformation under AFM cantilever compression. This parameter appears to be important for modeling non-Laplacian systems of significant viscoelastic contributions, such as biological cell membranes or polymer blends.

INTRODUCTION

Emulsions are widely encountered in a variety of industries, including food processing, formulation of cosmetics, manufacture of pharmaceuticals, materials processing, and oil production. For some applications, stable emulsions are desirable. For instance, well-dispersed oil-in-water (milk) and water-in-oil (facial creams) emulsions are necessary to extend the shelf life of consumer products. However, emulsions encountered in the oil industry require rapid phase separation to remove water and associated ions from oil, thus improving product quality and minimizing the potential for equipment corrosion and fouling downstream processing. Emulsion stability strongly depends on the characteristics of the interface separating the dispersed and continuous phases. Partitioning of surface-active agents such as surfactants, polymers, and nanoparticles can influence the interactions between two approaching droplets as well as droplet deformation.[1−3]

In emulsion systems, hydrodynamic forces corresponding to the momentum of two interacting droplets contribute to the overall interaction force. In addition, as the distance between droplets decreases, surface forces including van der Waals and electrical double layer force become more significant and determine whether the droplets coalesce or remain dispersed. These forces contribute to the overall disjoining pressure of the intervening liquid film. Other surface forces such as hydration, hydrophobic, steric,

depletion, and/or bridging forces can be dominant in determining the stability of the intervening liquid film, depending on the nature of the system, which includes the presence of surface active species and/or polymers residing at or near the liquid−liquid interface. [2]

AFM has been extensively used to study nanoscale forces between rigid surfaces. Knowing the spring constant of the AFM cantilever, the magnitude of the force as a function of separation distance between rigid surfaces can be readily obtained. This measurement is achieved by calibrating the optical pass of laser detecting systems, using the slope of the constant compliance region where cantilever deflection has a linear dependency on piezo displacement. [4] Such an approach becomes invalid for determining interaction forces involving deformable surfaces. To understand interactions between two deformable interfaces in emulsion systems or between biological cells, researchers have previously measured interaction forces between two solid substrates coated (deposited or adsorbed) with surface-active species or biomolecules. Combined with theoretical modeling, these measurements have shed light on interactions between emulsion droplets stabilized by surface active species.[5] The scaling theory developed by de Gennes, for example, has been used to describe steric hindrance between polymer brushes responsible for steric stabilization.[6,7] However, establishing a direct link between the measured interaction forces using "model" emulsion surfaces and bulk emulsion stability is difficult, if not impossible, due to the deformable nature of the system. Deformable surfaces are also known to be more sensitive to interaction forces compared to rigid solid surfaces.[2]

To address this critical issue, pioneering AFM work by Butt[8] and Ducker[9] demonstrated the feasibility of direct force measurements for bubble−particle systems using a scanning probe microscope. Since these influential studies, a variety of complex interfaces have been investigated. Force measurement for particle−bubble/droplet systems using AFM is nontrivial, since both the cantilever and bubble/droplet can deform under surface forces and/or compression by the AFM cantilever. In such systems, the contact area between the particle and bubble/droplet changes as the colloidal probe is pressed down on the interface.[10] Interpretation of the corresponding force curves is further complicated by the presence of surface active species, which add yet another deformable layer to the system.[7] Since interfacial deformation occurs prior to contact, due to an extended range of surface forces, there is no sharp transition between noncontact and contact regions. In such systems, zero separation between solid and droplet or bubble surfaces cannot be determined in the same way as for rigid bodies.[5,11] Other methods such as confocal microscopy or theoretical modeling are required to obtain "true" separation between the probe and droplet/bubble. When an AFM probe approaches a droplet, the droplet will deform when the disjoining pressure exceeds the Laplace pressure. Therefore, instead of reducing the distance between the solid−fluid interface (as is the case for solid−solid interaction), the droplet will deform (flatten) while the separation distance remains constant during further movement of the probe toward the droplet.[10]

In some cases of measuring interactions between solid probe and liquid droplets or bubbles, particle "snap-in" upon approach is observed, establishing a three-phase contact line where interactions are dominated by capillary forces.[11−13] However, when surfactants are present, fluid "wrapping" around the particle or dimple formation is more commonly observed, with a thin liquid film of the continuous phase remaining between the two surfaces without three-phase contact.[14−16] Force measurements between titania particles and air bubbles in electrolyte solutions at different pHs highlighted the effect of surface charge in flotation.[17] A large adhesion force was observed for pHs between isoelectric points of titania and bubble, a system where an attractive electrostatic interaction exists due to opposite surface charges. In contrast, weak adhesion was measured at pHs above the isoelectric point of titania. Experiments between air bubbles and mica in aqueous solutions demonstrated no bubble attachment to hydrophilic mica, while jump-in was recorded for partially hydrophobized mica.[18]

Droplet deformation has been experimentally shown by a reduction in slope of the constant compliance region of the force curves, which provides a qualitative comparison between systems, where higher slopes

indicate a more rigid or "solid-like" interface. In early studies, bubbles and deformable bodies were described as linear Hookean springs. [9] The complex spring constant of the system, which correlates with interfacial tension, was calculated from the constant compliance region of the force−displacement curve. [16,19] However, detailed theoretical investigation using the augmented Stokes−Reynolds−Young−Laplace (SRYL) equation showed the nonlinear behavior of force (F) versus interfacial tension (γ), and accurate quantitative predictions were achieved by the Chan−Dagastine−White model. [20] The augmented SRYL equation is a type of equation of state (EOS) which relates droplet or bubble deformation to the applied force, analogous to Hooke's law for springs. The assumptions required for this model include Stokes flow of the liquid between interacting surfaces and a boundary condition for the interface, with the drop shape described by the Young−Laplace equation. Although tangentially immobile or mobile boundary conditions can be applied for the various interfaces, the tangentially immobile condition produces a better fit in the majority of the studies due to the presence of impurities even in "clean" systems.

The SRYL model has been successfully applied to predict deformation for a number of systems with low Reynolds (Re) and Capillary (Ca) numbers, and to calculate the force exerted on the probe by the disjoining pressure from the interface as a function of separation distance. [18] In addition to film thickness, the augmented SRYL equations were used to predict the shape of droplets or bubbles, such as the formation of a "pimple", "dimple", or "wimple" from the spatial variation of the hydrodynamic and disjoining pressures due to surface and capillary forces. [21] By including the electrical double layer and van der Waals interactions in the disjoining pressure term, good agreement between experimental data and calculated forces has been shown for two decane droplets in aqueous systems of different electrolyte concentrations. [21] To predict interactions between two oil droplets with adsorbed polymer layers in electrolyte solutions, a steric term accounting for compression of the adsorbed polymer brushes was found essential to be incorporated into the disjoining pressure. [22] Interaction forces for two surfactant-free oil droplets (toluene) in electrolyte solutions could also be well fitted by the classical DLVO theory. However, additional steric interactions had to be included in the presence of natural polyaromatic molecules (NPAMs) of surface active nature, such as asphaltenes, present in petroleum oil. [23] In addition to the type and concentration of NPAMs in crude oil, stability of oil droplets in aqueous solution is also significantly influenced by the pH, as well as the type and concentration of ions in the aqueous phase. Good agreement between the calculated and measured drop deformations and magnitude of measured forces has been demonstrated for a variety of clean interfaces and polymer-covered droplets. [10,20−25] Ultimately, one can successfully predict droplet deformation on the basis of the force applied, provided that the size and boundary conditions of the particle and droplet are known. It should be noted that most oil−water deformable interface studies consider oil droplets in water, with few studies investigating interactions between water droplets in oil, an important system for many industrial applications. [26]

The augmented SRYL model assumes that the mechanical response of the bubble or droplet is dominated by interfacial tension and Laplace pressure.[20] However, Laplacian shape of the droplet upon deformation may not always be maintained when surface active species, such as proteins and particles, are irreversibly partitioned at the interface. For such systems, the surface may exhibit a significant restoring force under shear, i.e., an elastic interface that resists the change in area.[27,28] This solid-like behavior is manifested in many systems as "crumpling" or wrinkle formation upon droplet volume reduction.[29] In this case, elasticity has to be included to differentiate surface energy as observed in "solid-like" systems from surface tension for "fluid-like" systems.

The current study demonstrates the need to include interfacial elasticity in the augmented SRYL model in order to accurately predict the deformation of water droplets under the compression force of the AFM probe in an oil containing NPAMs (asphaltenes), that are soluble in toluene and less soluble in 50 Heptol.[30] It should be noted that the NPAMs encompass a wide range of molecular structures. Some of the NPAMs are permanently trapped at the interface, while others may be mobile to escape the interfaces during interface deformation. The overall properties of the interface come from the net effect of NPAMs,

with the major contributions from the irreversibly adsorbed interfacially active species. By taking advantage of self-assembly of NPAMs at the oil−water interface, we are able to form interfacial films of variable elasticities due to the continual adsorption/association (structuring) of NPAMs at the interface.[31] In previous studies, the interfacial film formed by NPAMs has shown a progressive and time-dependent rheological property, transitioning from a viscous dominant interface at short aging times to elastically dominant responses with longer aging.[30−35] Upon reduction of droplet volume, the interface is seen to crumple.[29] This elastic interfacial film often leads to poor water separation in petroleum emulsions by inhibiting droplet coalescence.[7,29,32−37] However, such time dependence and irreversibility of NPAM adsorption/self-assembly at the oil−water interface provide an opportunity to study the applicability of the augmented SRYL model predicting interfacial compressibility and interaction forces of a solid probe interacting with a water droplet in petroleum oil that progressively migrates from a Laplacian to a non-Laplacian response. Extending the existing SRYL equations to non-Laplacian interfaces is the focus of this study.

MATERIALS AND METHODS

Materials Preparation. Vacuum distillation feed bitumen was kindly provided by Syncrude Canada Ltd. High-performance liquid chromatography (HPLC)-grade toluene and n-heptane (Fisher Scientific) were used as solvent (toluene) or to prepare 50 Heptol (a mixture of 50:50 vol % n-heptane and toluene). Deionized water with a resistivity of 18.2 MΩ cm was prepared with an Elix 5 system, followed by purification with a Millipore-UV plus system. Silicon wafers were purchased from NanoFab (University of Alberta) and used as substrates. Tipless silicon nitride cantilevers were purchased from Bruker Scientific (Camarillo, CA) and used for the force measurement. Silica microspheres (D ≈ 8 μm) were purchased from Duke Scientific Co. (Palo Alto, CA) and glued to the tipless cantilevers to form colloidal probes.

Precipitation of Natural Polyaromatic Molecules (Asphaltenes) and Solution Preparation. Details on precipitation of asphaltenes, a class of natural polyaromatic molecules (NPAMs), have been described elsewhere.[38] Briefly, vacuum distillation feed bitumen was diluted with HPLC-grade toluene at a toluene/bitumen volume ratio of 5:1. The mixture was centrifuged at 35000g for 30 min to remove fines, usually mineral solids. Toluene was then allowed to evaporate from the diluted bitumen in a clean fume hood for 1 week to obtain solids-free bitumen. The NPAMs (asphaltenes) were extracted from the solids-free bitumen by adding n-heptane at an n-heptane-to-bitumen volume ratio of 40:1. The mixture was agitated for 2 h to achieve full precipitation, followed by gravity settling to separate the precipitates from the remaining solution. After settling, the supernatant was removed. To wash away the trapped solvent, the precipitates were repeatedly washed by adding additional n-heptane−shaking−settling until the supernatant appeared clear. The remaining n-heptane trapped in the precipitates of the final washing was then allowed to evaporate. The resulting precipitates of NPAMs accounted for 13 wt % of the original bitumen sample. Fresh solutions of NPAMs in toluene or 50 Heptol were prepared prior to each experiment by dissolving NPAMs in the desired solvent under sonication in an ultrasonic bath for 15 min.

Preparation of Cantilever and Substrate. A silica sphere (D ≈ 8 μm) was glued onto either a long wide-beam or a short narrow-beam AFM cantilever (model NP-O10) at its apex location using a two-component epoxy (EP2LV, Master Bound, Hackensack, NJ). The modified cantilevers were placed in a vacuum desiccator for 24 h, after which the probes were exposed to an ultraviolet light for 1 h to remove organic contaminants from the silica sphere (probe). The spring constant of the modified cantilever was measured prior to and after AFM force measurements and did not show any significant change over the course of the measurements (<5%). The spring constants for the long wide-beam and short narrow-beam modified cantilevers were in a range of 0.12−0.22 N/m. For a given system, equivalent and reproducible force profiles were obtained using both the long wide- beam and short narrow-beam cantilevers. Silicon wafers, used as substrates, were first treated with piranha solution for 1 h to remove impurities. The

cleaned wafers were then soaked in 1 mM octadecyltrichlorosilane (OTS) (ACROS Organics, Geel, Belgium) in toluene solutions for 30 s to partially hydrophobize the surfaces. The substrates were then rinsed with copious amounts of toluene and gently dried with nitrogen gas. This procedure resulted in an intermediate contact angle of 45−50° measured through the water droplet in air. Wafers of intermediate hydrophobicity were required to keep water droplets immobilized on the substrate in NPAM solutions during AFM measurements.

AFM Force Measurements. Interactions between a silica sphere and a water droplet in NPAM solutions were measured using an Agilent 5500 Molecular Imaging Microscope (Agilent Technologies Inc., Chandler, USA). Force profiles were collected in NPAM-in- toluene or 50 Heptol solutions using the vendor-provided liquid cell. The experimental setup for the measurement of probe−droplet interaction forces is shown in Figure 1a. Also shown in this figure is a top view optical microscope image of the cantilever positioned over a water droplet (shown in the inset) in NPAM solution. After adding 0.5 vol % water to the freshly prepared NPAM solution, the mixture was sonicated for 5 s. The resulting emulsion was slowly injected into the AFM liquid cell using a glass pipet. In our AFM system, the static electricity interference was not observed. The water drop size on the treated substrate obtained using this method was of a diameter range of 60−100 μm. The cantilever was then positioned over a selected droplet (D ≈ 70 μm) and allowed to approach the interface. The set point of the AFM was kept at 0 V, and the piezo travel distance was constant at 4 μm during force measurements. Since the "true" separation between the probe and droplet cannot be determined due to droplet deformations under cantilever load and the nontransparent nature of the system, the measured force in this study is plotted as a function of unprocessed piezo displacement. In AFM measurements, only the distance between "hard" substrates is known, i.e., between the probe and underlying substrate. Other complementary techniques, such as confocal microscopy[25] or theoretical calculations using the SRYL model,[21] are required to obtain "true" separation between a probe and a soft interface. Cantilever velocity was kept at 1 μm/s in order to avoid the effect of hydrodynamics.[10] Figure 1b shows the piezo displacement as a function of time. A single AFM force profile was acquired in 8 s. Deflection sensitivity and spring constant values of the colloidal probe against the underlying OTS-treated substrate were calculated prior to and after force measurements using the Thermal K function available in Agilent 5500 AFM software. All measurements were carried out at room temperature (24 °C). One limitation of this experimental setup is that the NPAM concentration in the continuous phase has to remain fairly low (≤0.1 g/L), as the solution should be sufficiently translucent to obtain a high laser sum and reduce scattering. The Agilent 5500 AFM is equipped with an environmental chamber, suitable for measurements using volatile organic solutions as in our case. However, even with the seals in place, measurements were kept to a maximum of 1 h for toluene and 30 min for 50 Heptol solutions to minimize any effect that might result from solvent evaporation.
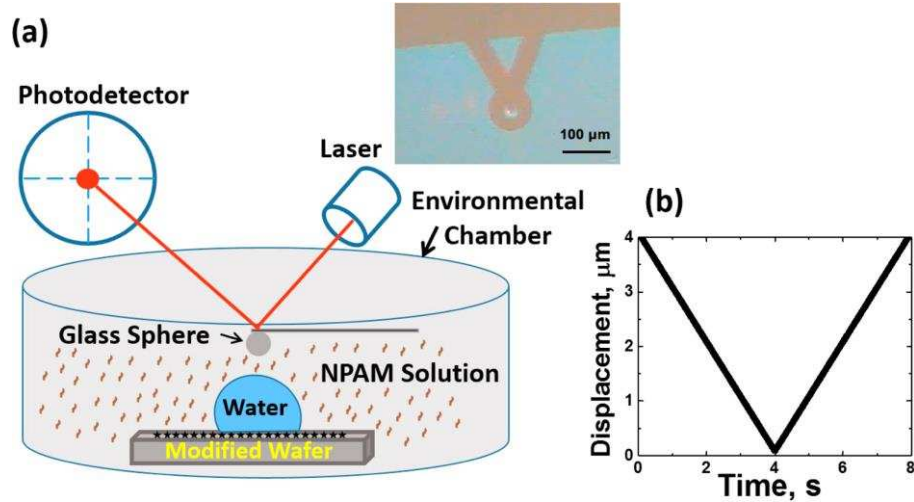
Figure 1. (a) Experimental setup for measurement of interaction forces between a silica sphere (D ≈ 8 μm) and water droplet (D ≈ 70 μm) in 0.1 g/ L NPAM solution. (b) AFM piezo movement as a function of time. The inset shows the top view of the AFM cantilever positioned over a selected water droplet on the treated substrate NPAM solution. Note that the glued glass sphere is on the underside and hence not visible using the top view camera.

Measurement of the Contact Angle, Interfacial Tension, and Crumpling Ratio. Interfacial characterization studies were conducted using a Theta Optical Tensiometer T200 (Biolin Scientific, Stockholm, Sweden) at room temperature (24 °C). The contact angle of water droplets on untreated hydrophilic substrates soaked in NPAM solution was measured in air. Similar measurements were made on the OTS-treated substrates in air, toluene, 50 Heptol, as well as 0.1 g/L NPAM-in-toluene or 50 Heptol solutions. For measurements in air, a water droplet (V ≈ 9 μL) was carefully placed on the substrate and contact angle measured for 3 min at 3 fps. For measurements in NPAM solutions, a fresh solution was prepared prior to each measurement. The treated substrate was placed in a rectangular quartz cell, and a water droplet (V ≈ 9 μL) was deposited on the substrate and brought into focus. The NPAM solution was then added to the cell mimicking the setup used for the force measurement using the AFM probe technique. The time-dependent contact angle was recorded over 60 min (3 fps), a time span comparable to the AFM force measurement. All the experiments were repeated three times, and the error was within 5%.

Prior to each interfacial tension and crumpling ratio measurement, fresh NPAM solution was transferred into a rectangular quartz cell and a water droplet (D ≈ 2 mm) was generated from a 1 mL gastight Hamilton syringe with an 18-gauge needle (Reno, NV). The droplet profile was recorded and analyzed using the Theta software. The tensiometer camera was calibrated prior to each experiment, and droplet images were recorded at 12 fps for 60 min. The tests were repeated a minimum of three times for each condition with the measurement error less than 10%. Edge detection was used for pendant drop shape analysis and the interfacial tension was determined using the Young−Laplace equation. The interfacial tension relates to the drop shape by

$$\gamma = \Delta\rho g \frac{R_0^2}{\beta} \qquad (1)$$

where γ is the interfacial tension, Δρ is the density difference between fluids, g is the gravitational acceleration constant, R0 is the radius of drop curvature at the apex, and β is the shape factor.

Crumpling of the water droplet was measured in 0.1 g/L NPAM solutions to demonstrate the development of viscoelastic interfacial film[39] by deviation of a water droplet from its pendant shape in response to volume reduction.[40] To measure the crumpling ratio, a water droplet (V ≈ 6 μL) was generated at the tip of an 18-gauge needle in NPAM solution and allowed to age for up to 1 h (0, 5, 15, 30, 60 min), after which the droplet volume was slowly reduced at a rate of 50 μL/min until "folds" or "crumpling" was observed at the interface. The crumpling ratio is defined as the apparent area of the droplet prior to crumpling (A_f) divided by the initial droplet area (A_i):[40]

$$CR = \frac{A_f}{A_i} = \frac{\pi R_f^2}{\pi R_i^2} \qquad (2)$$

With the CR defined as such, a large CR would indicate a more rigid interface.

Dilatational Rheology. There are different methods to follow the development of interfacial elasticity. Forth et al., for example, studied the development of interfacial elasticity by tracking the drop shape of constant volume and calculating the discrepancy between the predicted shape by the Young−Laplace equation and the measured drop shape.[41] In the current study, the more conventional oscillatory pendant drop method was used to quantify the interfacial dilatational elasticity. The pulsating droplet module (PD 200) of the Theta Optical Tensiometer T200 was used to measure dilatational viscoelastic complex modulus (E) and hence the dilatational elastic modulus (E′) of the NPAM-stabilized oil−water interface. A water droplet of V ≈ 5−6 μL was formed at the tip of an 18-gauge needle in 0.1 g/L NPAM solution (toluene or 50 Heptol), and sinusoidally oscillated to vary the drop volume and hence interfacial area. The tracking of interfacial tension and area during a given measurement is shown in the Supporting Information (Figure S1).
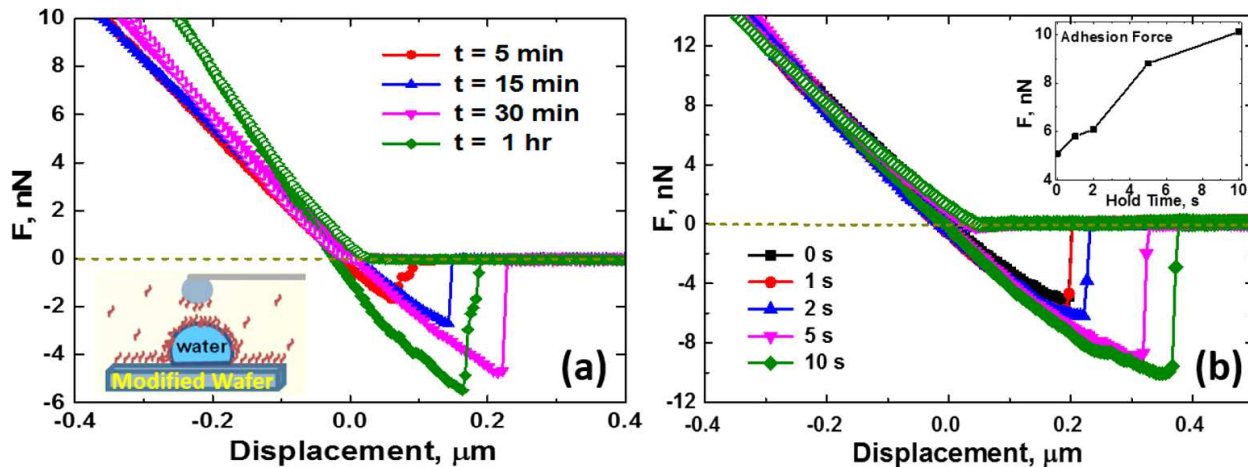

Figure 2. (a) Interactions between silica probe (D ≈ 8 μm) and water droplet (D ≈ 70 μm) in 0.1 g/L NPAM-in-toluene solutions upon cantilever approach (open symbols) and retract (filled symbols), as a function of droplet aging time. (b) Effect of cantilever "hold time" on the adhesion force between the colloidal probe and a NPAM-stabilized interfacial layer formed at the oil−water interface (D ≈ 75 μm) after 30 min. The inset shows the adhesion force magnitude versus hold time.

Dependence of E on oscillation frequency is linked to characteristics of the relaxation process of NPAMs at the interface. Since the freshly created expanding interface is exposed to the bulk phase for a longer period of time, diffusion controlled adsorption occurs at low frequencies, in contrast to intrinsic elasticity at higher frequencies.[32] However, due to hydrodynamic effects associated with the oscillation, this

method loses accuracy at high frequencies.[42] For NPAM-stabilized interfaces, a good frequency range was determined to be 0.1−0.5 Hz. In the current study, the droplet volume change was set to be 10% during sinusoidal oscillation, and the frequency of oscillation was set at 0.1 Hz. Each measurement of the interfacial viscoelasticity was comprised of 10 oscillations with a 10 s delay. The complex viscoelastic modulus E can be separated into E′ (elastic modulus) and E″ (viscous modulus) through the well-established relationship[42−47]

$$E = \frac{\Delta\gamma}{\Delta A/A_0} = E' + iE'' = E' + 2\pi i\nu\mu \qquad (3)$$

where $\Delta\gamma$ is the change in interfacial tension, ΔA is the amplitude, A0 is the reference area, E′ is the dilatational elasticity, E″is the loss (viscous) modulus, i is the imaginary unit, ν is the oscillation frequency, and μ is the viscosity of the droplet liquid. For the systems considered, the viscous modulus was found to be very low (1−2 mN/ m) and did not change over time. Therefore, only the elastic modulus is reported in this study.

RESULTS AND DISCUSSION

Interaction Forces between a Rigid Sphere and Deformable Interfaces in Organic Solvents.
Interaction forces between a silica sphere and a micron-sized water droplet in NPAM solutions were measured using AFM to probe oil− water interfacial aging. Figure 2a shows the time-dependent interaction forces between a silica sphere (D ≈ 8 μm) and water droplet (D ≈ 70 μm) immersed in 0.1 g/L NPAM-in-toluene solution for up to 1 h. A higher slope in the "high force" constant compliance region implies a more rigid or "solid-like" interface, which is readily observed as the interface ages. The slope of the constant compliance region increases from 27 mN/m at aging time t = 5 min to 41 mN/m at t = 1 h. The time-dependent change in the slope of the constant compliance region is mainly due to adsorption/association of NPAMs at the oil−water interface. This time-dependent change was shown in our previous study as an increase in the extended range of repulsion over time when the interaction forces were measured between two mica surfaces in similar NPAM solutions using SFA.[48] On approach, the nature of the interaction forces between the two surfaces in NPAM-in-toluene solutions is purely repulsive, attributed to steric repulsion of swollen NPAM layers on silica and/or the oil−water interface. It is interesting to note a significant increase in the adhesion force (and force range) during cantilever retraction as the cantilever "hold time" at the interface is increased (Figure 2b) and the intervening film is given more time to drain. When the interfacial materials (aggregates) become compressed as the colloidal probe moves toward the interface, an increase in interpenetration and bridging of NPAMs/aggregates is anticipated, which accounts for the observed increase in adhesion upon probe retraction. Since the electrical double layer is negligible in the nonaqueous environment, the forces of interaction for the system of interest are attributable to steric and van der Waals forces.

For 50 Heptol (see the Supporting Information, Figure S2), the aging effect was found to be less pronounced and the interfacial deformation and force magnitude did not change significantly during 30 min aging. This reduced time dependency in 50 Heptol is likely due to a much faster adsorption and/ or association of NPAMs in 50 Heptol than in toluene on solids and at the oil−water interface, which will be discussed further in the following sections. Since the interfacial stiffening occurred mostly during the first colloidal probe approach to the interface (approach time ∼5 min), only one representative force curve at 15 min aging time will be discussed further. The AFM force measurements were stopped after 30 min aging in order to minimize the change in solution composition due to a higher evaporation rate of heptane over toluene. Measuring further interfacial stiffening at longer aging times in NPAM-in-50 Heptol solution would be extremely interesting once the limitation of possible composition change in the AFM liquid cell is resolved.

SRYL Prediction for Droplet Deformation. To better understand and predict the measured changes in drop deformation, the high force formula of the augmented SRYL equations was applied to our system. With proper boundary conditions, the Chan−Dagastine−White model has been successfully used to predict the equilibrium force (F) as a function of relative piezo displacement (ΔD) for interactions between a particle and a bubble/droplet or between two bubbles or droplets. [10,20,21] This model utilizes the augmented SRYL equations to predict film drainage and deformations based on the force applied. It should be emphasized that this model applies the Young−Laplace equation for droplet shape, which is accurate only for "fluid-like" systems of minimal viscoelasticity. By using the high force equation with a specified boundary condition of the augmented SRYL model (eqs 4−6), droplet deformation under given loads can be accurately predicted.[21]

$$\Delta D(y) \equiv \frac{F(t)}{4\pi\sigma}\left[\ln\left(\frac{F(t)R_{ds}}{8\pi\sigma R_O^2}\right) + 2B(\theta) - \frac{4\pi\sigma}{K} - 1\right] \qquad (4)$$

$$B(\theta) = 1 + \frac{1}{2}\ln\left[\frac{1+\cos(\theta)}{1-\cos(\theta)}\right] \qquad (5)$$

$$R_{ds} \equiv \frac{1}{\left[\frac{1}{R_O}+\frac{1}{R_S}\right]} \qquad (6)$$

where ΔD is the predicted displacement, F(t) is the measured force, R_{ds} is linked to R_O and R_s, the radii of the unperturbed droplet and sphere, respectively, θ is the contact angle of the droplet on the substrate in solution, σ is the interfacial tension, and K is the spring constant of the cantilever.

The extent of droplet deformation depends on the boundary conditions selected, which could be either a pinned three-phase contact line or constant contact angle as the probe is pressed on the droplet. Considering the much smaller size of the probe than the droplet and small displacement of the probe in our experiment, the deformation of the interface in the context of drop volume can be considered negligible to ensure a pinned three-phase contact line given by eq 5.

Water droplet contact angles in toluene on wafers of different hydrophobicity can be found in the Supporting Information (Figure S3). The selected intermediate contact angle of 50° in air resulted in contact angles of 86 and 74° in NPAM-in-toluene and 50 Heptol solutions, respectively, with the droplet firmly anchored on the substrates.

AFM imaging of the substrate surface features revealed that NPAMs adsorbed on the substrate within 15 min, and no significant change was observed at longer exposure times (Figure S4). Surface properties and roughness of the underlying OTS-treated substrates were also checked prior to and after force measurements for each system (Table S1). The SEM images presented in the Supporting Information (Figure S5) confirmed that the contact area of the silica sphere did not change upon exposure to NPAMs. Therefore, by considering the results in Figures S3−S5, one can conclude that the changes in slopes of the constant compliance region of force curves reported in Figure 2a are indeed due to the changes in the physical properties of the oil/water interface.

To apply the augmented SRYL model to the force profiles as a function of droplet aging time, shown in Figure 2, the dynamic interfacial tension (σ(t)) of the system needs to be determined. The measured dynamic interfacial tension of a water droplet in 0.1 g/L NPAM-in-toluene and 50 Heptol solutions is shown in Figure 3. For a clean oil−water interface, baseline interfacial tensions of 36 and 43 mN/m were measured for water−toluene and water−50 Heptol, respectively. A rapid decrease in the interfacial tension of water in contact with NPAM solutions was observed within the first 10 min for both solutions, indicating a rapid adsorption of the interfacially active material. This initial rapid decrease in interfacial tension was followed by a slower secondary decay which is often associated with reorganization and relaxation of NPAMs at the oil−water interface.[49] After 15 min of aging time, the interfacial tensions for

both systems equaled 26.8 mN/m, and slowly approached a steady-state value of ~24.5 mN/m after 1 h. However, the initial slope of interfacial tension versus time is quite different for the two solutions, indicating a significant effect of solvent aromaticity on interfacial activity of NPAMs.
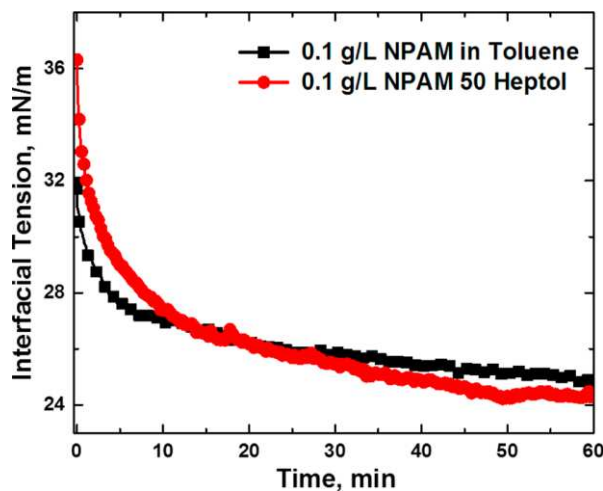

Figure 3. Interfacial tension of a water droplet in 0.1 g/L NPAM-in-toluene or 50 Heptol solution.

Using the dynamic interfacial data, the measured forces acting upon the colloidal probe during approach (system: NPAM-in-toluene solution at 15 min and 1 h water droplet aging) are compared with the predictions from the theoretical model in Figure 4. The model provides a good fit for the force profile at a short aging time, t = 15 min, but deviates from the experimental result at a longer aging time of 1 h. Since B(θ), Rds, and K are constant during the droplet aging, as shown in the Supporting Information (Figures S3 and S4 and Table S1), and σ decreases only by ~2 mN/m from 15 min to 1 h of aging, as shown in Figure 3, the observed deviation of the measured force profiles by the model at longer aging times cannot be explained by considering only the change in interfacial tension. For interfaces of substantial viscoelasticity due to the highly cross-linked nature of interfacially active NPAMs, as in the current study, the extent of deformation could be greatly influenced by interfacial rheology. For such systems, it is not surprising that the current SRYL model could not predict droplet deformation and interaction force, as the NPAMs irreversibly partitioned at the interface exhibit a significant restoring force under shear. To understand the observed deviation, a closer look at the interfacial properties is therefore warranted.

Development of Viscoelasticity at the Oil−Water Interface. To illustrate the cross-linking of NPAMs and "stiffening" of the interface, the time-dependent crumpling ratio of a water droplet aged in NPAM solutions (toluene and 50 Heptol) was determined. The results in Figure 5 show that for both solvents the crumpling ratio increases with increasing interfacial aging, indicating an increased resistance of the interface to in-plane shear. Interfacial crumpling upon droplet volume reduction demonstrates the development of a mechanical barrier at the interface and deviation from a classical Laplacian response. Crumpling occurs due to the irreversible adsorption of NPAMs at the oil−water interface, [49] as a critical interfacial concentration is eventually reached during droplet contraction to cause "jamming" of the interfacial network. For crumpling to occur, the compressional elasticity should be nonzero while the interfacial shear elasticity should be significant. [50]
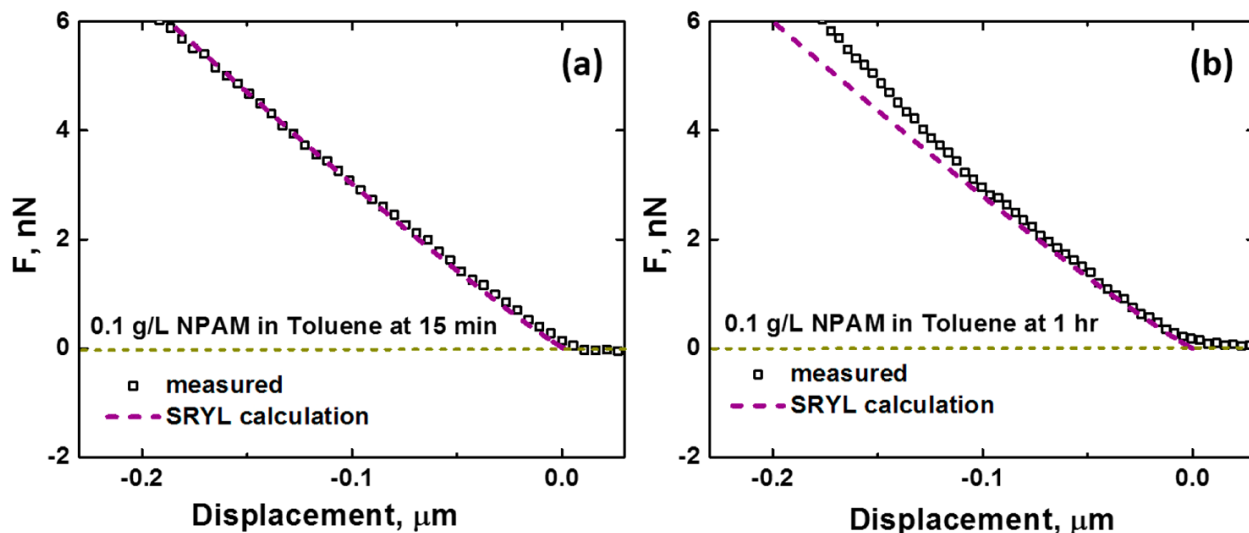
Figure 4. Comparison of measured forces over the constant compliance (high force) region (symbols) in 0.1 g/L NPAM-in-toluene solution upon approach at (a) 15 min and (b) 1 h with the predictions from the SRYL model (dashed lines).

Development of a rigid "skin" and hence deviation from Laplacian shape can qualitatively explain the lack of agreement between the measured and predicted forces by the existing SRYL equation after 1 h of aging, as shown in Figure 4b.
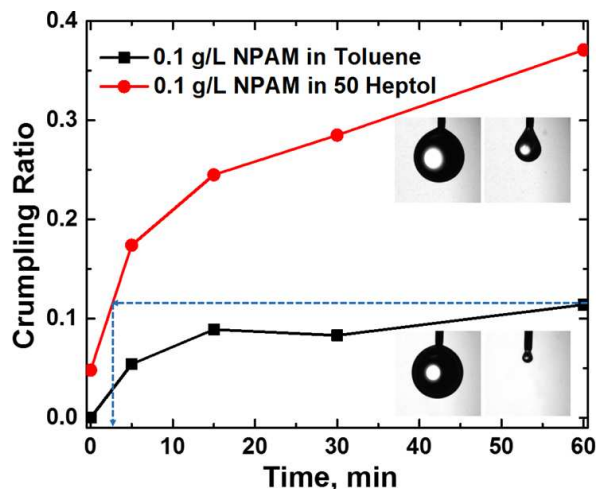

Figure 5. Crumpling ratio of water droplets aged in NPAM-in-toluene and 50 Heptol solutions. The images shown in the inset compare the initial water droplet shape and that at the onset of crumpling after 1 h of interfacial aging.

For 0.1 g/L NPAM-in-toluene solution, the crumpling ratio (CR) after 1 h of droplet aging was 0.12, indicating interfacial crumpling at an 88% reduction in drop volume. For 50 Heptol, the crumpling ratios are higher compared to toluene at equivalent aging times, with CR = 0.37 after 1 h of droplet aging. However, due to the AFM setup limitations, force measurements at an equivalent time could not be conducted. The force curve after 15 min of aging time in 50 Heptol NPAM solution is equivalent (if not slightly more rigid) compared to the corresponding toluene case after 1 h of aging time, as indicated in Figure 5. A higher crumpling ratio in 50 Heptol indicates that the interfacial film is more resistant to

compression and hence more rigid than the film formed in toluene. Higher crumpling ratios in poorer solvents correlate well with the findings from earlier studies showing that NPAM molecules are most effective at stabilizing emulsions in "poorer" solvents (~50 Heptol) when NPAM concentration is below the critical precipitation concentration.[34] It is interesting to note that, while the interfacial tensions for both toluene and 50 Heptol systems are similar at 15 min and 1 h of aging time, the crumpling ratios are considerably different with CR50 Heptol > CR toluene. This finding confirms that interfacial tension alone cannot fully describe changes occurring at the oil−water increases with increasing droplet aging, indicating the formation of more "solid-like" and mechanically stronger interfacial films. A higher dilatational elasticity is measured for an interfacial film formed in 50 Heptol. This finding is consistent with higher crumpling ratios (Figure 5) and relates to faster interfacial adsorption dynamics (Figure 3) and stronger intermolecular interactions between NPAMs in poorer solvents. It is evident that the ability to form a cohesive interlinking network is enhanced in less aromatic solvent. Previous research investigating surface forces between NPAM deposited/adsorbed on mica showed an increased attraction and stronger adhesion forces of NPAMs in Heptol than in toluene. [7]
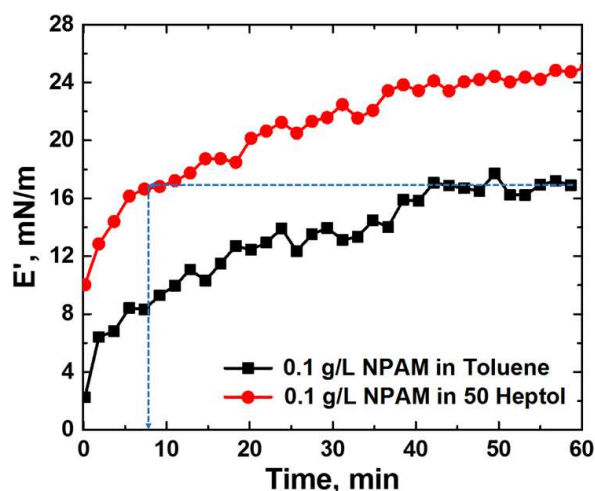

Figure 6. Time-dependent dilatational elastic modulus for a water droplet aged in NPAM solutions.

Such rapid adsorption of NPAMs from 50 Heptol as shown in Figures 3 and 6 explains the lack of time-dependent changes in the 50 Heptol force curves (see Figure S2), as a rapid increase in the interfacial elasticity to ~16 mN/m occurs in the first 5 min. As indicated in Figure 6, it takes an equivalent of 1 h of aging for NPAM-in-toluene solution to reach the same level of interfacial elasticity. Our interfacial characterization studies confirm that NPAMs adsorb at the oil−water interface to form strongly elastic films which exhibit resistance to in-plane shear (non-Laplacian behavior). The dynamics of this process are accelerated in "poorer" solvents (50 Heptol) due to the increase in interfacial activity and stronger interaction between NPAM aggregates. While these characteristics are often probed on planar surfaces or millimeter size droplets, the research described in this study demonstrates the potential of AFM to measure such dynamic interfacial changes and the requirement to account for the interfacial elasticity in the widely used high force droplet deformation equation of the augmented SRYL model.

Viscoelasticity Correction Factor to Modify the High Force SRYL Equation. For complex interfaces where deviation from Laplacian behavior occurs and interfacial crumpling is observed, the Young−Laplace equation does not provide a good approximation for droplet shape. When crumpling is observed, interfacial tension/surface energy (σ) should not be substituted for surface stress (τ), similar to that observed for solid surfaces.[27,28,51] Gibbsian formulation of thermodynamics of interfaces given below is more representative of the case, i.e.,

$$\Delta p = \tau \left(\frac{1}{R_1} + \frac{1}{R_2} \right) \qquad\qquad (7)$$

where Δp is the increment in pressure and R1 and R2 are local radii of curvature. With the replacement $\tau = \sigma$, eq 7 simplifies to the Young−Laplace equation. However, this replacement is allowable only for interfaces of non-viscoelastic nature.[27] For solid-like surfaces and similarly for interfaces with elasticity and surface strain ε, the surface stress tensor given by eq 8 instead of surface tension (equivalent to surface energy) should be used.[28]

$$\tau = \sigma + \frac{\partial \sigma}{\partial \varepsilon} \qquad\qquad (8)$$

As shown in Figure 4b, the slope of the constant compliance region at 1 h aging time is higher than that predicted by the existing SRYL model, indicating a more "rigid" interface. This mechanical stiffness as the colloidal probe is pushed against the interface can be addressed by inclusion of a viscoelastic correction factor (σ/E' indicated by eq 8) inside the brackets in eq 4. As a result, the high force formula (eq 4) becomes

$$\Delta D(y) \equiv \frac{F(t)}{4\pi\sigma} \left[\ln\left(\frac{F(t)R_{ds}}{8\pi\sigma R_0^2} \right) + 2B(\theta) - \frac{4\pi\sigma}{K} - 1 + \frac{\sigma}{E'} \right] \qquad\qquad (9)$$
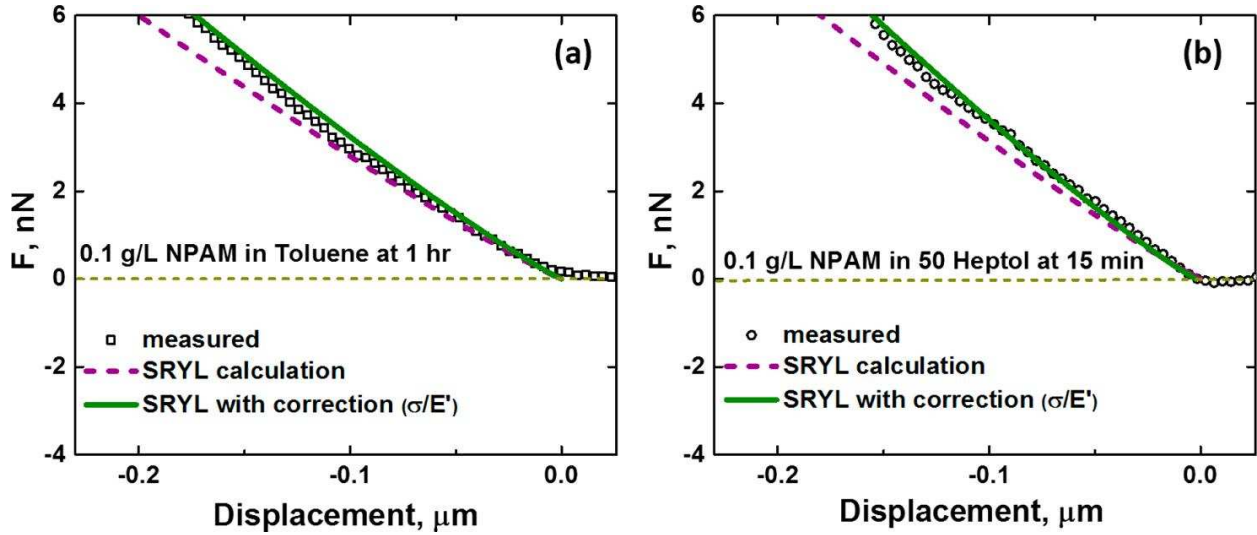

Figure 7. Measured forces upon approach in 0.1 g/L NPAM solution (a) in toluene after 1 h of aging and (b) in 50 Heptol after 15 min of aging, plotted in comparison with predictions using the SRYL model (eq 4) and the modified SRYL model to account or interfacial elasticity (eq 9).

Applying the corrected formula (eq 9) to both systems that exhibit significant interfacial crumpling upon drop volume reduction (water droplet aging in 0.1 g/L NPAM-in-toluene solution at 1 h and in 50 Heptol solution at 15 min), the results in Figure 7 show a negligible discrepancy between experimental data and the theoretical prediction in the high force region during approach. It is interesting to note that for the toluene system after 1 h aging, the elasticity is 15.8 mN/m and the slope of constant compliance is 41 mN/m, while, for the 50 Heptol system after 15 min of aging time, the elasticity is 17 mN/m and the slope of constant compliance is 44 mN/m. Hence, independent of the solvent type, there is a very good agreement between the dilatational elasticity and the interfacial stiffness as measured under normal load deformation. The interplay between interfacial tension and interfacial elasticity is crucial for non-

Laplacian systems where deformation is not well-predicted by the high force equation of SRYL. As the deviation from Laplacian behavior increases, for example, due to higher cross-linking of molecules, interfacial rheology will play a more significant role in the interfacial dynamics. Tracking the changes in interfacial tension and interfacial elasticity explains the deviations from the traditional high force calculation and provides better predictions for droplet deformation, an important factor in emulsion stability.

CONCLUSIONS

In this study, interactions between a silica probe and a viscoelastic interface, formed by the continual accumulation of natural polyaromatic species at an oil−water interface, have been examined. Our system of interest showed progressive rheological aging of the interface, resulting in the formation of a rigid "skin" and quasi-solid-like behavior of a water droplet. The development of an interfacial mechanical barrier is a contributing factor to enhanced emulsion stability as a result of interfacial aging and decreased solvent quality. This non-Laplacian behavior leads to a discrepancy between the measured droplet deformation and that predicted by the SRYL equation in the "constant compliance" (high force) region. A viscoelastic correction term is introduced into the equation to account for the increased interfacial dilatational rheology. This critical modification is shown to provide excellent theoretical prediction of the deformation of an interface of non-Laplacian nature.

REFERENCES

(1) Wilde, P. J. Interfaces: their role in foam and emulsion behaviour. Curr. Opin. Colloid Interface Sci. 2000, 5 (3−4), 176−181.

(2) Krasowska, M.; Prestidge, C. A.; Beattie, D. A.; Dar, Y. L.; Light, J. M. Atomic force microscopy for determining surface interactions of relevance for food foams and emulsions. Food Texture Design and Optimization; John Wiley & Sons, Ltd: Chichester, U.K., 2014; pp 402−422.

(3) Langevin, D. Influence of interfacial rheology on foam and emulsion properties. Adv. Colloid Interface Sci. 2000, 88 (1−2), 209− 222.

(4) Butt, H. J.; Cappella, B.; Kappl, M. Force measurements with the atomic force microscope: Technique, interpretation and applications. Surf. Sci. Rep. 2005, 59 (1−6), 1−152.

(5) Gromer, A.; Penfold, R.; Gunning, A. P.; Kirby, A. R.; Morris, V. J. Molecular basis for the emulsifying properties of sugar beet pectin studied by atomic force microscopy and force spectroscopy. Soft Matter 2010, 6, 3957−3969.

(6) de Gennes, P. G. Polymers at interface; a simplified view. Adv. Colloid Interface Sci. 1987, 27, 189−209.

(7) Wang, S.; Liu, J.; Zhang, L.; Masliyah, J.; Xu, Z. Interaction forces between asphaltene surfaces in organic solvents. Langmuir 2010, 26 (1), 183−190.

(8) Butt, H. J. Technique for measuring the force between a colloidal particle in water and a bubble. J. Colloid Interface Sci. 1994, 166 (1), 109−117.

(9) Ducker, W. A.; Xu, Z.; Israelachvili, J. N. Measurements of hydrophobic and DLVO forces in bubble-surface interactions in aqueous solutions. Langmuir 1994, 10 (9), 3279−3289.

(10) Tabor, R. F.; Grieser, F.; Dagastine, R. R.; Chan, D. Y. C. Measurement and analysis of forces in bubble and droplet systems using AFM. J. Colloid Interface Sci. 2012, 371 (1), 1−14.

(11) Gillies, G.; Prestidge, C. A.; Attard, P. An AFM study of the deformation and nanorheology of cross-linked PDMS droplets. Langmuir 2002, 18 (5), 1674−1679.

(12) Gillies, G.; Prestidge, C. A. Colloid probe AFM investigation of the influence of cross-linking on the interaction behavior and nano-rheology of colloidal droplets. Langmuir 2005, 21 (26), 12342−12347.

(13) Nguyen, A. V.; Evans, G. M.; Nalaskowski, J.; Miller, J. D. Hydrodynamic interaction between an air bubble and a particle: atomic force microscopy measurements. Exp. Therm. Fluid Sci. 2004, 28 (5), 387−394.

(14) Connor, J. N.; Horn, R. G. The influence of surface forces on thin film drainage between a fluid drop and a flat solid. Faraday Discuss. 2003, 123, 193−206.

(15) Chen, L.; Heim, L.-O.; Golovko, D. S.; Bonaccurso, E. Snap-in dynamics of single particles to water drops. Appl. Phys. Lett. 2012, 101, 031601.

(16) Filip, D.; Uricanu, V. I.; Duits, M. H. G.; Agterof, W. G. M.; Mellema, J. Influence of bulk elasticity and interfacial tension on the deformation of gelled water-in-oil emulsion droplets: an AFM study. Langmuir 2005, 21 (1), 115−126.

(17) Krasowska, M.; Carnie, S. L.; Fornasiero, D.; Ralston, J. Ultrathin wetting films on hydrophilic titania surfaces: equilibrium and dynamic behavior. J. Phys. Chem. C 2011, 115 (22), 11065−11076.

(18) Shi, C.; Chan, D. Y. C.; Liu, Q.; Zeng, H. Probing the hydrophobic interaction between air bubbles and partially hydrophobic surfaces using atomic force microscopy. J. Phys. Chem. C 2014, 118 (43), 25000−25008.

(19) Munz, M.; Mills, T. Size dependence of shape and stiffness of single sessile oil nanodroplets as measured by atomic force microscopy. Langmuir 2014, 30 (15), 4243−4252.

(20) Chan, D. Y. C.; Dagastine, R. R.; White, L. R. Forces between a rigid probe particle and a liquid interface: I. The repulsive case. J. Colloid Interface Sci. 2001, 236 (1), 141−154.

(21) Chan, D. Y. C.; Klaseboer, E.; Manica, R. Film drainage and coalescence between deformable drops and bubbles. Soft Matter 2011, 7, 2235−2264.

(22) Manor, O.; Chau, T. T.; Stevens, G. W.; Chan, D. Y. C.; Grieser, F.; Dagastine, R. R. Polymeric stabilized emulsions: steric effects and deformation in soft systems. Langmuir 2012, 28 (10), 4599−4604.

(23) Shi, C.; Zhang, L.; Xie, L.; Lu, X.; Liu, Q.; Mantilla, C. A.; van den Berg, F. G. A.; Zeng, H. Interaction mechanism of oil-in-water emulsions with asphaltenes determined using droplet probe AFM. Langmuir 2016, 32 (10), 2302−2310.

(24) Webber, G. B.; Manica, R.; Edwards, S. A.; Carnie, S. L.; Stevens, G. W.; Grieser, F.; Dagastine, R. R.; Chan, D. Y. C. Dynamic forces between a moving particle and a deformable drop. J. Phys. Chem. C 2008, 112 (2), 567−574.

(25) Tabor, R. F.; Lockie, H.; Mair, D.; Manica, R.; Chan, D. Y. C.; Grieser, F.; Dagastine, R. R. Combined AFM−confocal microscopy of oil droplets: Absolute separations and forces in nanofilms. J. Phys. Chem. Lett. 2011, 2 (9), 961−965.

(26) Vakarelski, I. U.; Li, E. Q.; Thoroddsen, S. T. Soft colloidal probes for AFM force measurements between water droplets in oil. Colloids Surf., A 2014, 462, 259−263.

(27) Shuttleworth, R. The surface tension of solids. Proc. Phys. Soc., London, Sect. A 1950, 63, 444−457.

(28) Cammarata, R. C. Surface and interface stress effects in thin films. Prog. Surf. Sci. 1994, 46 (1), 1−38.

(29) Yeung, A.; Dabros, T.; Masliyah, J. Dissipative interfaces and departures from the Young-Laplace equation. Langmuir 1997, 13 (24), 6597−6606.

(30) Harbottle, D.; Chen, Q.; Moorthy, K.; Wang, L.; Xu, S.; Liu, Q.; Sjoblom, J.; Xu, Z. Problematic stabilizing films in petroleum emulsions: shear rheological response of viscoelastic asphaltene films and the effect on drop coalescence. Langmuir 2014, 30 (23), 6730− 6738.

(31) Masliyah, J.; Zhou, Z. Z.; Xu, Z.; Czarnecki, J.; Hamza, H. Understanding water-based bitumen extraction from Athabasca oil sands. Can. J. Chem. Eng. 2004, 82, 628−654.

(32) Yarranton, H. W.; Sztukowski, D. M.; Urrutia, R. Effect of interfacial rheology on model emulsion coalescence I. Interfacial rheology. J. Colloid Interface Sci. 2007, 310 (1), 246−252.

(33) Yarranton, H. W.; Sztukowski, D. M.; Urrutia, R. Effect of interfacial rheology on model emulsion coalescence II. Emulsion coalescence. J. Colloid Interface Sci. 2007, 310 (1), 253−259.

(34) McLean, J. D.; Kilpatrick, P. K. Effects of asphaltene aggregation in model heptane−toluene mixtures on stability of water-in-oil emulsions. J. Colloid Interface Sci. 1997, 196 (1), 23−34.

(35) Langevin, D.; Argillier, J.-F. Adv. Colloid Interface Sci. 2016, 233, 83−93.

(36) Taylor, S. D.; Czarnecki, J.; Masliyah, J. Disjoining pressure isotherms of water-in-bitumen emulsion films. J. Colloid Interface Sci. 2002, 252 (1), 149−160.

(37) Jestin, J.; Simon, S.; Zupancic, L.; Barre, L. A small angle neutron scattering study of the adsorbed asphaltene layer in water-in-hydrocarbon emulsions: Structural description related to stability. Langmuir 2007, 23 (21), 10471−10478.

(38) Zhang, L. Y.; Lawrence, S.; Xu, Z.; Masliyah, J. H. Studies of Athabasca asphaltene Langmuir films at air-water interface. J. Colloid Interface Sci. 2003, 264 (1), 128−140.

(39) Woodward, N. C.; Gunning, A. P.; Maldonado-Valderrama, J.; Wilde, P. J.; Morris, V. J. Probing the in situ competitive displacement of protein by nonionic surfactant using atomic force microscopy. Langmuir 2010, 26 (15), 12560−12566.

(40) Gao, S.; Moran, K.; Xu, Z.; Masliyah, J. Role of bitumen components in stabilizing water-in-diluted oil emulsions. Energy Fuels 2009, 23 (5), 2606−2612.

(41) Forth, J.; French, D. J.; Gromov, A. V.; King, S.; Titmuss, S.; Lord, K. M.; Ridout, M. J.; Wilde, P. J.; Clegg, P. S. Temperature- andpH-Dependent Shattering: Insoluble Fatty Ammonium Phosphate Films at Water−Oil Interfaces. Langmuir 2015, 31 (34), 9312−9324.

(42) Rane, J. P.; Pauchard, V.; Couzis, A.; Banerjee, S. Interfacial rheology of asphaltenes at oil-water interfaces and interpretation of the equation of state. Langmuir 2013, 29 (15), 4750−4759.

(43) Miller, R.; Ferri, J. K.; Javardi, A.; Krağ el, J.; Mucic, N.; Wüstneck, R. Rheology of interfacial layers. Colloid Polym. Sci. 2010, 288 (9), 937−950.

(44) Pauchard, V.; Rane, J. P.; Banerjee, S. Asphaltene-laden interfaces form soft glassy layers in contraction experiments: A mechanism for coalescence blocking. Langmuir 2014, 30 (43), 12795−12803.

(45) Liggieri, L.; Santini, E.; Guzmań , E.; Maestro, A.; Ravera, F. Wide-frequency dilational rheology investigation of mixed silica nanoparticle−CTAB interfacial layers. Soft Matter 2011, 7, 7699− 7709.

(46) Ravera, F.; Loglio, G.; Kovalchuk, V. I. Interfacial dilational rheology by oscillating bubble/drop methods. Curr. Opin. Colloid Interface Sci. 2010, 15 (4), 217−228.

(47) Maldonado-Valderrama, J.; Rodríguez Patino, J. M. Interfacial rheology of protein−surfactant mixtures. Curr. Opin. Colloid Interface Sci. 2010, 15 (4), 271−282.

(48) Natarajan, A.; Kuznicki, N.; Harbottle, D.; Masliyah, J.; Zeng, H.; Xu, Z. Understanding mechanisms of asphaltene adsorption from organic solvent on mica. Langmuir 2014, 30 (31), 9370−9377.

(49) Freer, E. M.; Radke, C. J. Relaxation of asphaltenes at the toluene/water interface: Diffusion exchange and surface rearrangement. J. Adhes. 2004, 80 (6), 481−496.

(50) Erni, P.; Jerri, H. A.; Wong, K.; Parker, A. Interfacial viscoelasticity controls buckling, wrinkling and arrest in emulsion drops undergoing mass transfer. Soft Matter 2012, 8, 6958−6967.

(51) Erni, P. Deformation modes of complex fluid interfaces. Soft Matter 2011, 7 (17), 7586−7600.